

at all (see Table II). Thus, transient pores induced by the electrical breakdown are permeable to the molecular size up to naphthalene molecules but not to the large pyrene molecules. In the pulsation experiments of the planner lipid bilayer membranes, it is reported that the number of transient pores created during a short duration of the electrical breakdown is estimated to be  $10^7/\text{cm}^2$ , and the pore radius is calculated to be 4 nm.<sup>23</sup>

Molecular mechanisms responsible for the opening of transient pores are not yet clear. One may consider<sup>24</sup> that polar head groups of lipids are reoriented, which allows a rapid leakage of permeants under the electric field. When the bilayer is assumed to be elastic but incompressible,<sup>25</sup> the applied field induces a stress on the lipid bilayer and thins down the membrane. Consequently, the area per lipid must increase and such an expansion of the bilayer membrane may be responsible for the transient pores. Another interpretation of these pores is given by the analysis of electrical breakdown of planner lipid bilayers.<sup>26</sup> In that case, spontaneous pores exist in the membrane due to the structural defects whose development is favored by the electric field.

(23) Benz, R.; Zimmermann, U. *Biochim. Biophys. Acta* **1981**, *640*, 169.

(24) Seeling, J. *Q. Rev. Biophys.* **1977**, *10*, 353.

(25) White, S. H. *Biophys. J.* **1974**, *14*, 155.

(26) Abidor, I. G.; Arakelyan, V. B.; Chernomordish, L. V.; Chizmadzhev, Yu. A.; Pastushenko, V. F.; Tarasevich, M. R. *Bioelectrochem. Bioenerg.* **1979**, *6*, 37.

## Summary

Although nylon capsule membranes were simply semipermeable, the capsule corked with lipid bilayers could reversibly regulate the permeability by the external electric field. The transient pores induced by an electrical breakdown are reversibly generated for a long duration (3–5 min) in the corking bilayers and have a selectivity for the dye permeation. It is difficult, however, for liposomal membranes to realize the reversible permeation control and form transient pores for any long duration, because they are easily damaged or fused each other under the electric field. On the contrary, the bilayer-corked capsule membrane is not damaged by the continuous and intermittent electric field, because lipid bilayers are supported by the physically strong nylon capsule wall. The signal receptive permeability control induced by the electric field is reproducible and useful for a model of the synaptic systems in which a nerve electrical impulse initiates the rapid release of a chemical intermediary.

**Registry No.** 1, 97732-71-3; 2, 99646-32-9; 3, 130-14-3; 4, 1655-29-4; 5, 5182-30-9; 6, 59572-10-0; di-4-ASP, 101630-71-1;  $2C_{12}N^+2C_{11}$ , 3282-73-3;  $2C_{14}N^+2C_{11}$ , 68105-02-2;  $2C_{16}N^+2C_{11}$ , 70755-47-4;  $2C_{18}N^+2C_{11}$ , 3700-67-2;  $2C_{12}PO_4^-$ , 45300-74-1;  $2C_{16}PC$ , 18545-88-5;  $C_{12}BB-C_4-N^+$ , 101630-72-2;  $C_{12}Azo-C_4-N^+$ , 101630-73-3; NaCl, 7647-14-5;  $CaCl_2$ , 10043-52-4; *p*-Bu<sub>3</sub>NC<sub>6</sub>H<sub>4</sub>CHO, 90134-10-4; D-glucose, 50-99-7; 4-picolinium, 16950-21-3; nylon-2,12, 41510-72-9; nylon-2,12 SRU, 41724-60-1.

## Forces between Surfaces of Block Copolymers Adsorbed on Mica

Georges Hadziioannou,\*† Sanjay Patel,† Steve Granick,†† and Matthew Tirrell\*†

Contribution from the IBM Almaden Research Center, San Jose, California 95120, and the Department of Chemical Engineering and Materials Science, University of Minnesota, Minneapolis, Minnesota 55455. Received September 9, 1985

**Abstract:** Forces exerted between block poly(vinyl-2-pyridine)/polystyrene (PV2P/PS) copolymer layers adsorbed on mica substrates have been measured over the separation range 0–200 nm between the substrate surfaces. The PV2P block binds strongly to mica in a flattened configuration; the PS block is not bound directly to mica in our experiments. The PS block is held on the surface through its covalent bond to PV2P. The form and range of the force vs. separation curve depend upon block molecular weights and the thermodynamic quality of the immersion solvent for the PS chain. In the good solvent toluene, the PS chains are shown to be stretched away from the surfaces in extended configurations and to exert long-ranged, mutually repulsive forces when two layers are brought to a separation causing overlap of the PS chains. In the  $\theta$  solvent cyclohexane, the range is reduced considerably due to configurational contraction and due to the diminished effects of binary interactions between polymer segments. The range of the forces observed and their dependence on block molecular weights can be explained by fairly simple arguments about the packing of polymer chains on the surface.

Conformations of macromolecules adsorbed on solid surfaces immersed in solvent are, in general, altered significantly from conformations of polymers dissolved in the bulk of the solvent.<sup>2</sup> Instrumental tools available to study these conformations are limited in both number and capability. Ellipsometry gives a characteristic thickness and mean refractive index of an adsorbed layer on a reflective substrate.<sup>3</sup> Hydrodynamic measurements give a different characteristic length scale of the adsorbed configuration.<sup>4</sup> Neutron scattering<sup>5</sup> and fluorescence excited by evanescent waves through surfaces<sup>6</sup> promise to provide more complete data on the polymer segment density profile within adsorbed layers but at present are fraught with complexities in interpretation. Detailed understanding of the conformations of adsorbed macromolecules rests upon knowledge of the intermolecular forces between polymers and solid substrates and on how these forces are affected by environmental conditions such as

temperature and the thermodynamic quality of the immersion solvent.

(1) Permanent address: Polymer Group and Department of Ceramic Engineering, University of Illinois, Urbana, IL 61801.

(2) Takahashi, A.; Kawaguchi, M. *Adv. Polym. Sci.* **1982**, *46*, 1. This reference presents an excellent review of all experimental and theoretical results on the configurations of adsorbed polymers. Such a comprehensive review is therefore omitted from the current article.

(3) Kawaguchi, M.; Takahashi, A. *J. Polym. Sci., Polym. Phys. Ed.* **1980**, *18*, 2069.

(4) (a) Priel, Z.; Silberberg, A. *J. Polym. Sci., Polym. Phys. Ed.* **1978**, *16*, 1917. (b) Varoqui, R.; Dejardin, P. *J. Chem. Phys.* **1977**, *66*, 4395.

(5) (a) Barnett, K. G.; Cosgrove, T.; Vincent, B.; Burgess, A. N.; Crowley, T. L.; King, T.; Turner, J. D.; Tadros, T. F. *Polymer* **1981**, *22*, 283. (b) Barnett, K. G.; Cosgrove, T.; Vincent, B.; Sissons, D. S.; Cohen-Stuart, M. *Macromolecules* **1981**, *14*, 1018.

(6) (a) Allain, C.; Ausserré, D.; Rondelez, F. *Phys. Rev. Lett.* **1982**, *49*, 1694. (b) Ausserré, D.; Hervet, H.; Rondelez, F. *Macromolecules* **1986**, *19*, 85. (c) Ausserré, D.; Hervet, H.; Rondelez, F. *Phys. Rev. Lett.* **1985**, *54*, 1948. (d) Bloch, J. M.; Sansone, M.; Rondelez, F.; Peiffer, B. G.; Pincus, P.; Kim, M. W.; Eisenberger, P. *Phys. Rev. Lett.* **1985**, *54*, 1039.

\* IBM Almaden Research Center.

† University of Minnesota.

We have been working with an instrumental technique that gives information both on the conformations of adsorbed macromolecules and on the forces at play in the surface layer. We measure directly the force ( $F$ ) as a function of distance ( $D$ ) between two polymer layers adsorbed on smooth substrate surfaces. The technique enables us to determine force–distance profiles with precision of about 0.1  $\mu\text{N}$  in the force and 0.2 or 0.3 nm in the separation between the substrate surfaces. Precision of this quality is achieved by using as substrate surfaces molecularly smooth sheets of the aluminosilicate mineral Muscovite mica, in our surface forces apparatus of the design developed by Israelachvili,<sup>7</sup> described further in the Experimental Section.

The present work is on adsorbed layers of block copolymers, specially synthesized for these model experiments. Block copolymers may be viewed as macromolecular amphiphiles and have several important advantages and interesting characteristics for fundamental studies of adsorption. They can be synthesized, as we have done here, so that one block adsorbs strongly in a flattened conformation and the other block adsorbs negligibly. In particular we are studying diblock copolymers with one tightly bound poly(vinyl-2-pyridine) block (PV2P) and a polystyrene block (PS) that does not adsorb on mica in certain solvents that are good solvents for polystyrene in bulk, for example, toluene<sup>8</sup> (which is not to say that PS does not adsorb on mica immersed in any of its good solvents). One of the thrusts of this block copolymer study is exactly on this point; we want to study the behavior of adsorbed PS layers under environmental conditions where homopolymerized PS cannot itself be adsorbed on mica. A second point is perhaps less evident; by varying the molecular weight of the PV2P block, and thus the area on the mica surface taken up by the flattened PV2P conformation, we can vary the surface density of PS chains which are dangling away from the mica surface. With strongly bound PV2P blocks, a PS block is attached to the mica surface near its terminus. Polystyrene attached in this way bears some resemblance to a surface/chain end-grafted polymer that is anchored but does not adsorb itself. The control of surface density by the size of the PV2P block is akin to the control of the morphology of assemblies of surfactants and other low molecular weight amphiphiles by the size of the surfactant head group. A complete study of the effect of PV2P block molecular weight is in progress and will be published subsequently.

Here, we focus on the conformations and interactions of the polystyrene block. Direct measurements have been made previously<sup>9–11</sup> of force vs. separation profiles between saturated adsorbed layers of polystyrene on mica immersed in cyclohexane (CH). Individual segments of polystyrene adsorb weakly under these conditions, but PS adsorbs irreversibly overall, due to the cumulative effect of many simultaneously bound segments. The temperature where the second virial coefficient is zero, the  $\theta$  temperature,  $T_\theta$ , for solutions of polystyrene in cyclohexane is 34 °C. All previous measurements of forces between polystyrene adsorbed layers have been made in the vicinity of  $T_\theta \pm 10$  °C. The main features of the  $F(D)$  profiles near  $T_\theta$  have been discovered<sup>9,10</sup> and are general for a range of molecular weight. Below  $T_\theta$ , the two surfaces begin to exhibit mutual attraction at  $D$  of two to three times  $R_g$ ,<sup>12</sup> the radius of gyration of PS in bulk cyclohexane

Table I. Block Copolymer Characterization

sample designation	copolymer characteristic				
	PS $M_{w,sec}$	PS copolymer $M_w/M_{n,sec}$	PV2P $M_{w,LS}$	PV2P $M_{w,calcd}$	% w/w PS
60/60	60 000	1.09	120 000	60 000	0.50
60/150	185 500	1.22	240 000	54 500	0.77

<sup>a</sup>Sample designations refer to number average molecular weight of PV2P/PS blocks, respectively, in thousands (sec means obtained via size exclusion chromatography; LS via light scattering).

solution. This attraction increases in magnitude with decreasing  $D$  until about  $D \approx R_g$ . At this separation, there is an attractive minimum. At smaller  $D$  the force between the surfaces becomes strongly repulsive. Klein was the first to observe this pattern<sup>9</sup> and suggested that the attraction could be explained by the entry, with decreasing  $D$ , of the average concentration of polymer between the two surfaces into the two-phase region of the bulk PS–CH phase diagram. That this could not be the complete explanation was demonstrated by Israelachvili et al.,<sup>10</sup> who measured  $F(D)$  for PS layers immersed in CH above  $T_\theta$  (and therefore also above the critical consolute temperature). They found strong, though diminished, attractive forces exerted between the layers above  $T_\theta$ . This means that the attraction can neither be due exclusively to osmotic effects resulting from the negative second virial coefficient below  $T_\theta$  nor to entry into a two-phase region between the surfaces.

Israelachvili et al.<sup>10</sup> also observed a diminution of the range of the  $F(D)$  curve with increasing temperature, suggesting that the saturation monolayer adsorbance on mica decreases with increasing temperature. This fact, later supported by additional experimental  $F(D)$  data,<sup>11</sup> between submonolayer-covered mica where further *enhancement* of the attractive minimum is seen with diminished adsorbance, led Israelachvili et al.<sup>10</sup> to suggest that “bridging”, simultaneous adsorption of an individual macromolecule on both surfaces, is an important source of attraction, in addition to polymer segmental interactions in the presence of solvent. These segmental interactions would not be expected to produce attraction above  $T_\theta$ . However, bridging could produce attraction as long as adsorption is possible, which is, in general, well above  $T_\theta$ . Two alternative theories for these near- $T_\theta$  attractive force curves have been produced, based on a lattice theory<sup>13</sup> and on Cahn–Hilliard theory, respectively.<sup>14</sup> Both include, although by different means, the effect of bridging; both achieve a semi-quantitative prediction of the observed  $F(D)$  behavior.

While the bridging mechanism of attractive forces is very plausible, it has to date been difficult to probe directly. One of the difficulties is that our technique obviously requires the polymer layer to be adsorbed on mica. If a homopolymer adsorbs, it can also bridge, so that it is manifestly difficult to separate experimentally the effects of segmental and bridging attractions.

Block copolymers are a tool to this end. One block anchors the polymer and coats the mica surface; the other had little or not tendency to adsorb and, even if it has some small tendency to adsorb, it is strongly impeded by the anchoring block. Using the PV2P/PS block copolymers, we present results here on force vs. distance curves between PS layers attached in this way and immersed in the good solvent toluene. We thus eliminate bridging and measure for the first time forces between bound PS layers in a good solvent. We then return to the near- $T_\theta$  condition (by exchanging toluene for cyclohexane) for the PS block and study the purely thermodynamic segmental interaction between PS layers in CH in the absence of bridging.

## Experimental Section

**Synthesis and Characterization of Poly(vinyl-2-pyridine)/Polystyrene (PV2P/PS) Block Copolymers.** Anionic polymerization under inert gas is the technique we employ in order to obtain polymers of well-defined, uniform chemical structure. This method has been exploited extensively for homopolymers.<sup>15,16</sup> Systematic studies of the anionic co-

(7) Israelachvili, J. N.; Adams, G. E. *Nature (London)* **1976**, *262*, 774.  
(b) Israelachvili, J. N.; Adams, G. E. *J. Chem. Soc. Faraday Trans. 1* **1978**, *74*, 975.

(8) Luckham and Klein have examined forces between poly(ethylene oxide) (PEO) layers adsorbed on mica immersed in the good solvent for PEO, toluene: (a) Klein, J.; Luckham, P. F. *Macromolecules* **1984**, *17*, 1041. (b) Luckham, P. F.; Klein, J. *Macromolecules* **1985**, *18*, 721. They do not observe power law behavior; however, they do observe important and interesting nonequilibrium relaxation effects over the entire  $F(D)$  range they studied, so it is uncertain that their results are comparable to ours.

(9) (a) Klein, J. *Nature (London)* **1980**, *288*, 248. (b) Klein, J. *J. Chem. Soc., Faraday Trans. 1* **1983**, *79*, 99. (c) Almog, Y.; Klein, J. *J. Colloid Inter. Sci.* **1985**, *106*, 33.

(10) Israelachvili, J. N.; Tirrell, M.; Klein, J.; Almog, Y. *Macromolecules* **1984**, *17*, 204. It was also noted in this paper that  $T_\theta$  in a very narrow gap may be different from  $T_\theta$  in bulk.

(11) Granick, S.; Patel, S.; Tirrell, M. *Bull. Am. Phys. Soc.* **1985**, *30*, 539.

(12)  $D$ , in this paper, refers always to the separation between the bare mica substrate surfaces.

(13) Scheutjens, J. M. H. M.; Fleer, G. J. *Macromolecules* **1985**, *18*, 1882.

(14) (a) Klein, J.; Pincus, P. *Macromolecules* **1982**, *15*, 1129. (b) Ingerent, K.; Klein, J.; Pincus, P. *Macromolecules*, in press.

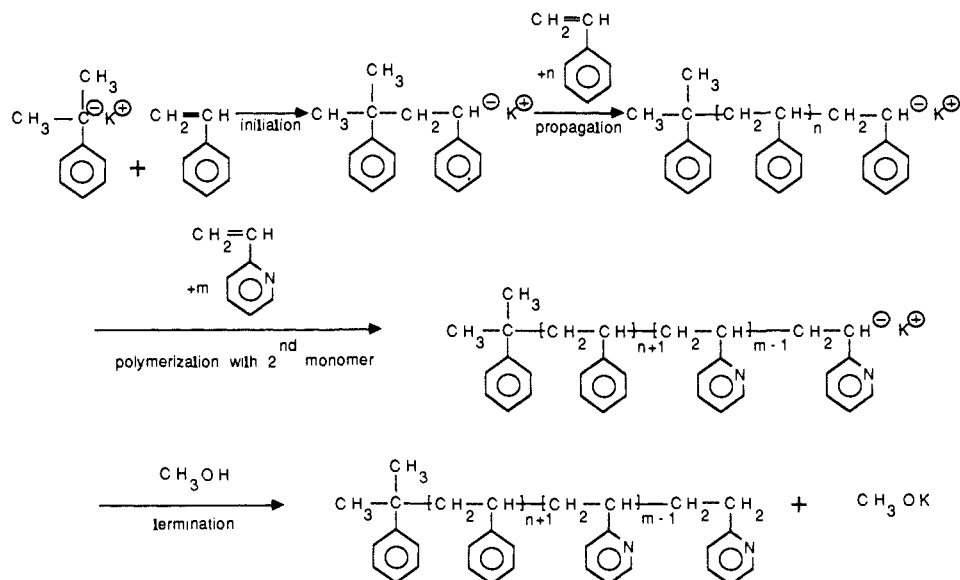


**Figure 1.** Synthesis scheme for PV2P/PS block copolymers. After complete styrene polymerization but before addition of vinyl-2-pyridine, a small aliquot of the reaction mixture is taken for molecular weight analysis of the PS block by SEC reported in Table I.

polymerization of styrene and vinyl-2-pyridine have been made by Sigwalt, et al.<sup>17-19</sup> and by Grosius et al.<sup>20</sup> Our choice was to use phenylisopropylpotassium as initiator<sup>21</sup> in the solvent tetrahydrofuran at low temperature ( $-70^{\circ}\text{C}$ ). The reaction scheme is illustrated in Figure 1. The relative amounts of initiator and monomers determine the molecular weights of the block. Monomers are added sequentially to the initiator in dilute solution in order to assure concentration homogeneity in the reaction medium. For the synthesis of PV2P-PS diblock copolymers, styrene was initiated first and allowed to polymerize to completion (exhaustion of styrene monomer), while maintaining the active polystyryl anion. A small quantity of this was removed from the reaction medium at this point, terminated with methanol, and reserved for subsequent molecular weight characterization of the PS block. Vinyl-2-pyridine monomer of the appropriate amount was then added to the reaction flask to attach a PV2P block of the desired molecular weight, which is then terminated with methanol.

This reaction scheme apparently avoids to a large extent certain parasitic side reactions noted by others. We have also investigated the method of Grosius et al.<sup>20</sup> of reducing the reactivity of the polystyryl anion in an effort to avoid side reactions, by reacting it with diphenyl-1,1'-ethylene before addition of vinyl-2-pyridine. No difference in properties was noted in the copolymers thus produced.

The molecular weight distributions of the polystyrene segments were determined via size exclusion chromatography (SEC) and the weight average molecular weights of the block copolymer were determined via light scattering (LS). The weight average and number average molecular weights,  $M_w$  and  $M_n$ , obtained from these analyses are summarized in Table I. The apparent average molecular weights of the block copolymers obtained by light scattering are essentially equal to the true weight average molecular weights of the copolymers since the refractive index increments,  $dn/dc$ , for PS and PV2P in tetrahydrofuran are nearly equal: 0.190 and 0.182, respectively. Anionic polymerizations such as we have used are expected to give blocks with narrow, Poisson distributions of molecular weight.<sup>15</sup> The data of Table I demonstrate the narrowness of the block length distributions, although the polydispersity of the sample with the higher molecular weight PS block, as measured by the ratio of weight to number average molecular weight from SEC, is slightly greater than anticipated on the basis of the Poisson distribution.

**Surface Forces Apparatus and Technique.** The measurements of the force as a function of separation between mica sheets bearing adsorbed layers of PV2P/PS block copolymers have been made on apparatus built according to the design developed by Israelachvili.<sup>7</sup> Although the apparatus has been described in detail, where the interested reader should

look for more complete information,<sup>7</sup> we believe that the technique has much more wide-ranging applications in chemistry than have yet been realized.

We therefore have presented in some detail, in the Supplementary Material, some background information on the technique,<sup>7,22-26</sup> including a schematic diagram of the apparatus, as well as our methods and protocol for using the apparatus. The design of the apparatus permits the direct measurement of interactions, as functions of separation, between surfaces held at separations from 300 nm down to contact.

**Materials.** The materials that are used in the experiment are an important part of the routine operation of the device. The mica used is Grade No. 4 ASTM V-2, clear and slightly stained Muscovite, ruby-red mica, which we obtain from Asheville-Schoonmaker Mica Co., Newport News, VA. All solvents, including toluene, cyclohexane, and ethanol, were spectroscopic grade (Fisher Scientific Co.) and distilled just prior to use. Doubly distilled water is used as part of the apparatus preparatory cleaning procedure. It is distilled after filtration, ion exchange, and contact with activated carbon.

**Procedure.** To reduce the risk of contamination, all parts of the apparatus that contact the liquid in the chamber are soaked overnight in 30% HNO<sub>3</sub> and then rinsed thoroughly with water. The various parts are then rinsed in filtered ethanol, blown dry with filtered nitrogen, and assembled in a laminar flow hood. The apparatus assembly is done in a separate laminar flow hood from that where the preparation of mica sheets is done by cleaving and cutting since the latter operation generates particulate debris in the form of mica flakes. Both laminar flow hoods operate at 99.999% efficiency for the removal of particles above 0.3  $\mu\text{m}$  in size. The mica pieces, cleaved and cut to  $\sim 0.002\text{ mm} \times 10\text{ mm} \times 10\text{ mm}$ , and silvered on one side, are glued on the glass disks, silvered side down. Many substances can be used as glue, provided they neither dissolve nor leach material that can contaminate the surfaces. For work in organic solvents, we favor a 50:50 by weight mixture of anhydrous reagent grade dextrose and galactose. This adheres well, has a convenient melting point, and shrinks little on cooling.

The assembled and sealed apparatus is mounted on a pneumatic vibration isolation table. At this stage, the bare mica surfaces are brought together in air to measure the thickness of the mica sheets and to ensure that strong, smooth adhesion occurs, indicating no contamination of the surfaces. Observation of contamination or debris at this point aborts the experiment.

Filtered toluene is then injected into the apparatus. The bare mica surfaces are brought together in toluene, and the experiment continued if no contamination or debris is found. Another check we make at this

(15) Swarc, M. "Carbanions, Living Polymers and Electron Transfer Processes"; Wiley-Interscience: New York, 1968.

(16) Morton, M.; Fetters, L. J. *J. Polym. Sci., Part D* **1967**, 2, 71.

(17) Champetier, G.; Fontanille, M.; Korn, A. C.; Sigwalt, P. *J. Polym. Sci.* **1962**, 58, 991.

(18) Fontanille, M.; Sigwalt, P. *Bull. Soc. Chim.* **1967**, 11, 4095.

(19) Fontanille, M.; Sigwalt, P. *C. R. Acad. Sci. (Paris)* **1960**, 251, 2947.

(20) Grosius, P.; Gallot, Y.; Skoulios, A. *Makromol. Chem.* **1969**, 127, 94.

(21) Asami, R.; Levy, M.; Szwarc, M. *J. Chem. Soc. (London)* **1968**, 58, 361.

(22) (a) Israelachvili, J. N.; Pashley, R. M. *Nature (London)* **1983**, 306, 249. (b) Pashley, R. M.; Israelachvili, J. N. *J. Colloid Inter. Sci.* **1984**, 101, 511.

(23) Tolansky, S. *Multiple Beam Interferometry of Surfaces and Films*; Oxford University Press: London, 1948.

(24) Israelachvili, J. N. *J. Colloid Inter. Sci.* **1973**, 44, 259.

(25) Derjaguin, B. V. *Kolloidn. Zh.* **1934**, 69, 155.

(26) Israelachvili, J. N.; Tabor, D. *Proc. R. Soc. (London)* **1972**, A331, 19.

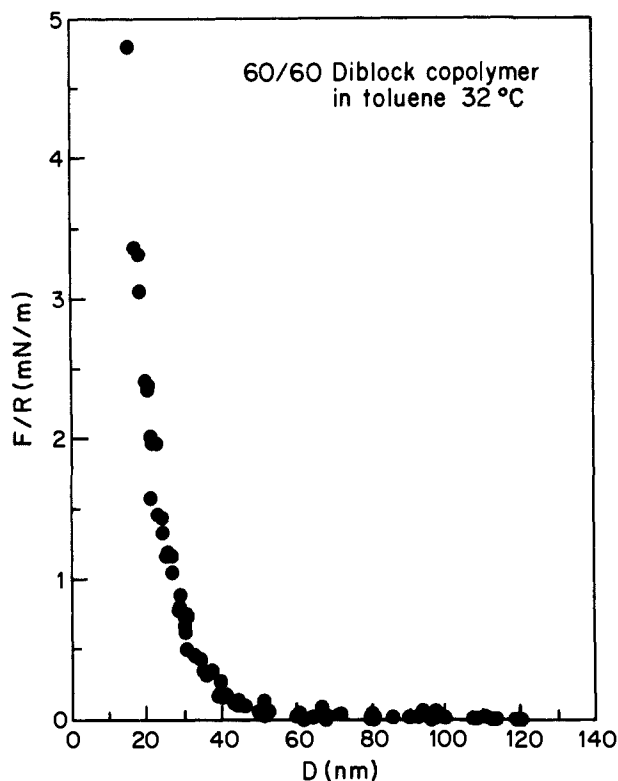


**Figure 2.** Force vs. distance for 60/60 PV2P/PS diblock copolymer layers in toluene.

point for purity and dryness of solvents like toluene and cyclohexane is to see that structural forces<sup>22</sup> in the range 1.0–5.0 nm are observed, indicating high purity. Filtered polymer solution is then injected into the apparatus, resulting in a typical final polymer concentration of  $70 \pm 5$   $\mu\text{g/mL}$ . The surfaces are then separated about 3 mm by means of the upper drive and adsorption of the PS/PV2P allowed to occur on the mica.

The adsorption in these experiments is allowed to occur to complete saturation, that is, until there are no further detectable changes in the adsorbed layer as monitored in the  $F(D)$  curve. PV2P/PS layer achieve a stable saturation within about 1 h. This rapid adsorption is in contrast to PS homopolymer adsorption on mica from cyclohexane, which we observe to require about 24 h for saturation stability. The more rapid kinetics of adsorption are evidently due to the strong binding of PV2P to mica. At this point we begin force vs. distance measurements. With this system, as with PS before,<sup>10</sup> it makes no detectable difference whether or not we replace the incubation polymer solution by pure toluene, presumably because we have a very dilute incubation solution and a very strongly bound polymer.

Temperature is controlled to  $\pm 0.5$  °C with a room temperature regulator. Thermal drifts are minimized by placing a styrofoam box around the apparatus and using IR filters on the white light measuring beam. For all conditions studied here, once a stable condition is achieved, it is maintained for 24–48 h during which time several  $F(D)$  curves are measured. An advantage of the crossed cylinder geometry is that the two surfaces can be moved relatively in order to examine several different contact areas. This is done routinely. When conditions of the experiment are changed, such as by changing temperature or solvent, a pre-equilibration period of up to 24 h is used to reattain stationary conditions. On changing solvent, large quantities of the new solvent are used to assure that there would be no residual old solvent of any significance remaining in the adsorbed layer.

All results reported here include data from two to four independent experiments. All of the force curves reported here for any chosen set of conditions (with one minor exception to be discussed) are identical whether measured with the two surfaces approaching or retreating from one other, are independent of delays between approach, retreat, and reapproach, and independent, so far as we can vary it, of the rate of approach or retreat. We therefore believe that all data reported here are close to equilibrium. All of the data presented in the figures of this paper are available in tabular form in the supplementary material in order to assist accurate theoretical modelling. This sort of check for dynamic effects is an essential part of the experimental procedure for this apparatus, especially with polymers, where important nonequilibrium effects have been observed under some circumstances.<sup>8</sup>

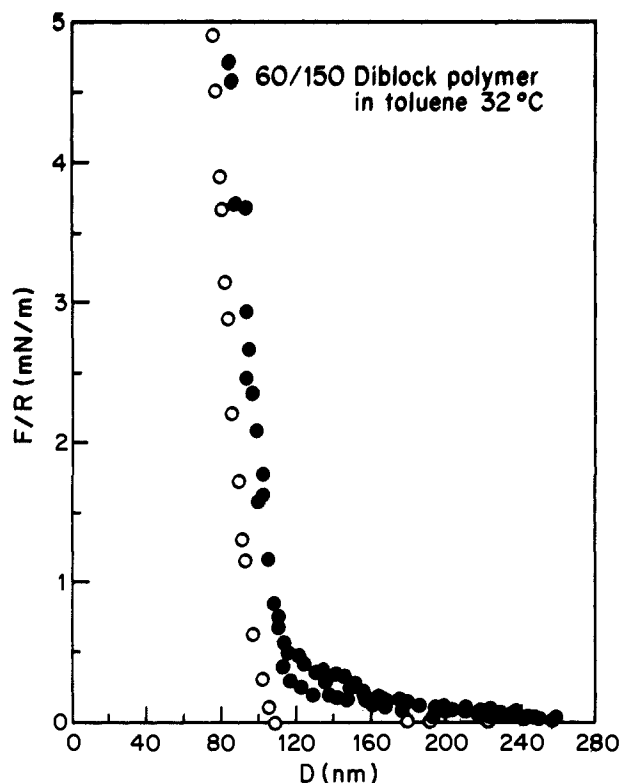


**Figure 3.** Force vs. distance for 60/150 PV2P/PS diblock copolymer layers in toluene. Open symbols refer to nonequilibrium data obtained under conditions described in the text.

## Results

Figures 2 and 3 present the data on  $F(D)$  for the two PV2P/PS block copolymers adsorbed on mica and immersed in toluene at 32 °C. (All of the data in this section in Figures 2–6 are available in tabular numerical form in the supplementary material.) The same qualitative features are exhibited by each curve. The interaction in toluene is purely repulsive and is long-ranged. Repulsive forces are detectable at separations equal to approximately ten times the radius of gyration of a free polystyrene chain of molecular weight equal to the PS block molecular weight in solution in toluene (approximately 7.0 nm for 60/60 and 11.1 nm for 60/150). This is in contrast to the situation with adsorbed homopolystyrene near the  $\theta$  temperature where the longest ranged detectable forces were at about  $3R_g$  of the polymer in free solution.<sup>10</sup> The repulsion here sets in more gradually at long range than in the near- $T_\theta$  case, where, once the force turns repulsive near  $D = R_g$ , it is very steep. The repulsions illustrated in Figures 2 and 3 are much less steep than for near  $T_\theta$  with homopolystyrene<sup>10</sup> even at comparable force levels, for example, around  $F/R = 2000$   $\mu\text{N/m}$ .

All of the data in Figures 2 and 3 represent equilibrium data, measured on both slow approaches and retreats, waiting between retreats and reapproaches, *except* for that data in Figure 3 indicated by the open symbols. For the 60/150 copolymer, we have observed nonequilibrium relaxation effects, *if* we squeeze the surfaces together to higher force values (e.g., 25 000  $\mu\text{N/m}$ ). If we squeeze to these high force values and wait an insufficient period between retreat and reapproach, we observe a curve such as the open symbols in Figure 3. These effects, which we have studied further and will be the subject of a future publication, are not seen for these polymers at force levels below 5000  $\mu\text{N/m}$  and we therefore exclude them from further consideration in this paper.

Direct comparison of the data of Figures 2 and 3 shows that a shift of a factor of 2.5 to 3 along the separation scale is needed to superimpose the two curves. This is larger than anticipated for a 2.5- to 3-fold difference in molecular weight on the PS blocks (see Table I). If the range of  $F$  scaled with molecular weight  $M$  like  $R_g$ , then we would expect a shift of about  $(2.5)^a$ , with  $a$  about

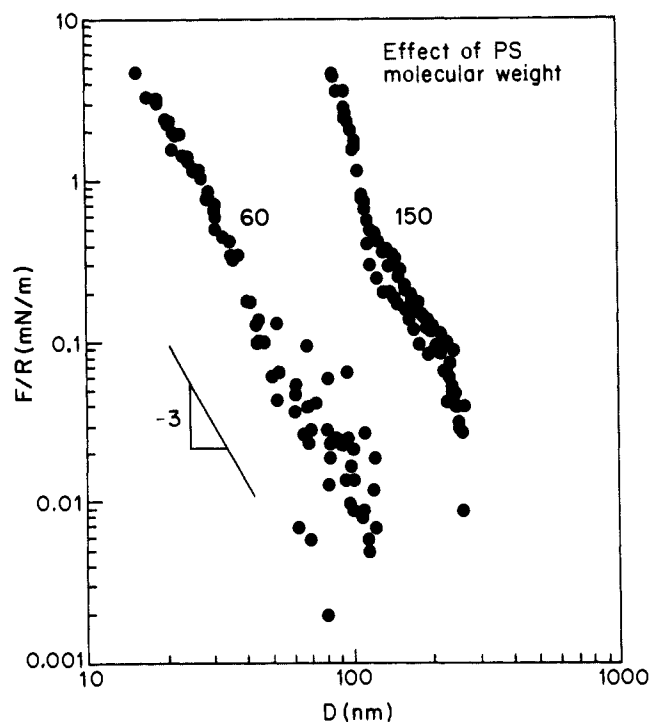


Figure 4. Double logarithmic plot of data in Figures 2 and 3: 60 refers to sample 60/60; 150 refers to sample 60/150.

0.6. In fact, we see that the range of  $F$  scales nearly linearly ( $a \approx 1$ ) with  $M$ . This point will be addressed in more depth in the Discussion; however, the high  $M$  dependence of the range of  $F$  and the magnitude of the range of  $F$  we observe, namely, about  $10R_g$  for 60/60, both suggest that the polystyrene blocks are extended away from the surface in configurations rather unlike random coils. For example, the extended contour length of a 60 000 molecular weight PS block can be estimated:  $600 \text{ repeat units} \times 0.25 \text{ nm/repeat unit} = 150 \text{ nm}$ . Therefore, the force first appearing at about 60 nm for the 60/60 copolymer come from PS blocks extended to about 20% of their mean contour lengths.

Figure 4 shows a log-log replot of the same data. Our precision of  $0.1 \mu\text{N}$  in force measurement corresponds to an estimated error of  $\pm 10 \mu\text{N/m}$  which accounts for the large scatter at the highest  $D$  in this representation. The data may conform to a power law but clearly not one of  $F(D) \sim D^{-2}$  as suggested by de Gennes<sup>27</sup> for the related but distinct case of irreversibly adsorbed homopolymer immersed in a good solvent. The  $F(D)$  data actually seem to vary more steeply than  $D^{-3}$  and not in a definitive power law fashion. There are clear reasons, given in the Discussion, why our experimental system may not accord with the assumptions of de Gennes' analysis.<sup>27</sup>

With this summary of the good solvent toluene results in hand, we turn to Figure 5 where the results of exchanging the immersion solvent for the 60/60 copolymer from toluene to the near- $T_\theta$  solvent, cyclohexane at 38 °C, are displayed. This is 3.5 °C above  $T_\theta$ , a temperature at which adsorbed layers of homo-PS on mica in cyclohexane are decidedly attractive,<sup>10</sup> with an attractive force of around  $-500 \mu\text{N/m}$ , depending on molecular weight. There is no evidence of attraction between the block copolymer layers under these conditions. The possibility of attraction between the layers due to bridging is negligible for these block copolymer layers

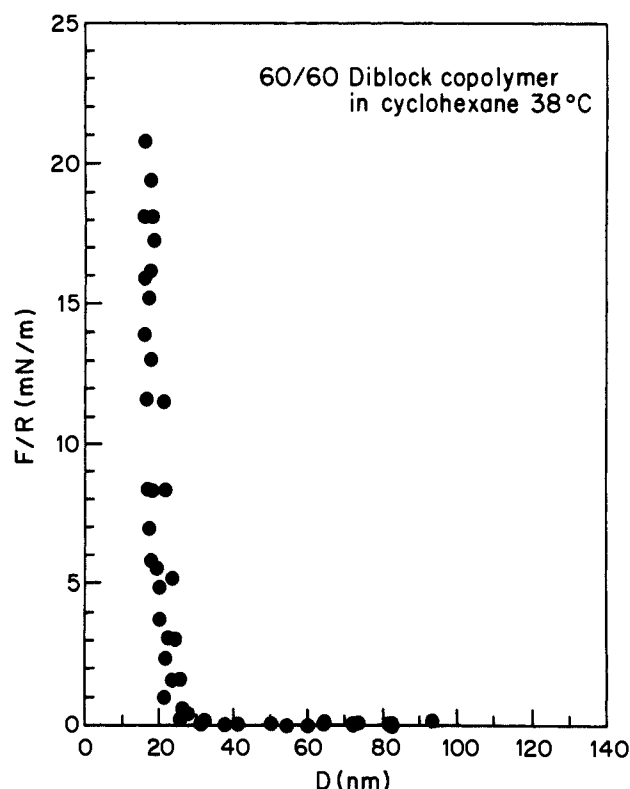


Figure 5. Force vs. distance for 60/60 PV2P/PS diblock copolymer layers in cyclohexane at 38 °C.

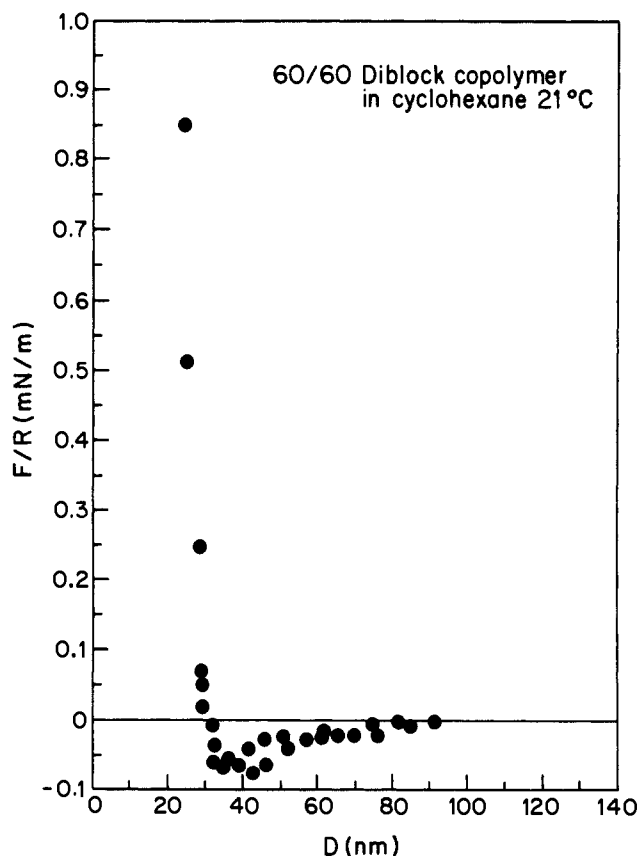


Figure 6. Force vs. distance for 60/60 PV2P/PS diblock copolymer layers in cyclohexane at 21 °C.

(27) (a) de Gennes, P.-G. *Macromolecules* **1981**, *14*, 1637. (b) de Gennes, P.-G. *Macromolecules* **1982**, *15*, 492. de Gennes predicts  $F \sim D^{-3}$  for flat plates; application of the Derjaguin treatment leads to the corresponding  $F \sim D^{-2}$  force law for orthogonal cylinders. The following references do treat forces between terminally attached chains but in the mean field manner appropriate for chains in near-random coil configurations. As discussed, this may not be an appropriate idealization for our experimental system. (c) Dolan, A. K.; Edwards, S. F. *Proc. R. Soc. (London)* **1974**, *A337*, 509. (d) Dolan, A. K.; Edwards, S. F. *Proc. R. Soc. (London)* **1975**, *A343*, 427. (e) Gerber, P. R.; Moore, M. A. *Macromolecules* **1977**, *10*, 476.

since the mica sites are blocked by PV2P and the layer was put on originally in toluene from which PS adsorbs negligibly on mica. The results of Figure 5 show that, even a few degrees above  $T_\theta$ , the purely osmotic (segmental mixing) part of the interaction between the layers is repulsive. Direct comparison of Figures 2

and 5 shows that the range of the repulsive force is substantially reduced on moving from a good solvent to near  $T_\theta$ . The longest ranged detectable repulsions occur at about  $10R_g$  in toluene and about  $4R_g$  in cyclohexane. The very steep repulsion at force levels of about  $5000 \mu\text{N/m}$  is similar in both cases and attains that level at about 13-nm separation in both cases. Onset of repulsion is much sharper in a poor solvent. The 13-nm separation locating the very steep repulsion is larger by a factor of more than 2 with this block copolymer than expected for homopolystyrene of 60000 molecular weight, again suggesting relative extension of the PS in the block copolymer layer even near  $T_\theta$ .

Figure 6 shows the effect of lowering the temperature well below  $T_\theta$  in CH. We now see unequivocal attraction appearing between the surfaces. The magnitude of the attraction between the block copolymer layers at 21 °C in CH is about  $-100 \mu\text{N/m}$ , in other words, some 5 to 10 times weaker than for PS homopolymer adsorbed under the same conditions. Repulsion appears at the same separation as in the higher temperature and better solvent cases.

### Discussion

The picture presented in Figures 2–4 is one where the copolymer adsorbs tightly from toluene by virtue of a sticky PV2P block whose surface density is such that the PS blocks extend from mica surface in somewhat stretched configurations. The fact that only repulsive forces are observed between these PS layers in the good solvent toluene is strong qualitative support for the notion that forces generated by osmotic pressure between the surfaces are the dominant effect in our experiments. Quantitative examination of the  $F(D)$  curves along these lines requires a theory for the osmotic pressure forces as a function of separation between the layers. This theory has been worked out only for adsorbed homopolymers that can bind to the surface at any segment along their contour.<sup>27</sup>

Our results on the ranges of the  $F(D)$  curves, and their scaling with molecular weight of the PS block, indicate that the configurations of, and therefore the segment density within, these PS blocks is different from that of comparably sized homopolystyrene. The segment density profile between the plates will determine, in turn, the osmotic pressure variation with separation.

The idealization of terminally grafted chains<sup>27c-e,28</sup> is closer than the case of homopolymer adsorption<sup>27a,b</sup> to our experimental situation. While the theoretical calculations for  $F(D)$  between two layers of high surface density, terminally grafted (but otherwise nonadsorbing) chains are not available,<sup>27c-e</sup> Alexander<sup>29</sup> and de Gennes<sup>28</sup> have analyzed the segment concentration profiles near one such surface. Gast and Leibler have pursued the analysis further.<sup>30</sup> This is clearly relevant to our discussion of the range of  $F(D)$  and its molecular weight dependence.

In the Alexander–de Gennes analysis,<sup>28,29</sup> the surface density,  $\sigma$ , of terminal attachments is a parameter that could be influenced in our experiments by PV2P block molecular weight. More exactly,  $\sigma$  is a dimensionless surface density equal to the number of terminally grafted chains per unit area times  $a^2$ , the area taken up by a single monomer segment. A particular density for terminally attached homopolymers is considered low if the coil domains of the attached chains do not overlap. For homopolymers at low  $\sigma$ , each chain occupies roughly a hemisphere of radius  $R_g$ . Low  $\sigma$  can then be defined:

$$\sigma < a^2/R_g^2 \quad (1)$$

or

$$\sigma a^2 R_g^2 < 1 \quad (2)$$

Since in a good solvent

$$R_g = N^{3/5}a \quad (3)$$

where  $N$  is the degree of polymerization, the condition for low surface density, becomes

$$\sigma < N^{-6/5} \quad (4)$$

This condition to achieve separate, rather normally configured chains at the surface is clearly quite low density for molecular weights of interest.

As  $\sigma$  becomes greater than  $N^{-6/5}$ , we expect chains to begin to adopt configurations extended away from the surface in order to accommodate the higher lateral packing along the surface. The Alexander–de Gennes argument proceeds along the following lines. At any  $\sigma$ , we can convert the surface density,  $\sigma a^{-2}$ , to an average distance on the surface between points of terminal attachment,  $\delta$ , thus

$$\sigma a^{-2} \equiv \delta^{-2} \quad (5)$$

or

$$\delta = a\sigma^{-1/2} \quad (6)$$

This  $\delta$  characterizes the extent of allowable lateral expansion of the chain. The chain will swell laterally in a blob of size  $\delta$  that contains some number of monomers,  $g$ , that is less than  $N$ .<sup>33</sup> The surface-grafted chain is assumed to extend away from the surface in a cylindrical zone filled by a string of blobs of radius  $\delta$ , whose number is  $N/g$ . The distance  $\delta$  between attachments is related to  $g$  via a relation for swollen coils in a good solvent like eq 3

$$\delta = g^{3/5}a \quad (7)$$

so that for  $\delta \ll R_g$ ,  $N/g$  will be large. The chains will be stretched out in a long string of blobs of size  $\delta$  so that over a significant distance the segment density,  $a^{-3}\Phi$ , where  $\Phi$  is the segment volume fraction, in the layer is constant and given by the number of monomers ( $g$ ) per unit volume ( $\delta^3$ ) of the blob:

$$a^{-3}\Phi = g\delta^{-3} \quad (8)$$

The thickness of the layer,  $L$ , which should determine the range of forces in our experiment, is readily estimated. The segment density,  $a^{-3}\Phi$ , must be equal to the total number of monomers ( $N$ ) per unit total volume of grafted chain ( $L\delta^2$ ):

$$a^{-3}\Phi = N/L\delta^2 \quad (9)$$

or using eq 6

$$a^{-3}\Phi = N/(La^2\sigma^{-1}) \quad (10)$$

and, finally, using eq 8, 7, and 6, it is seen that

$$L = Na\sigma^{1/3} \quad (11)$$

This gives the important result that, subject to the satisfaction of the several assumptions made in this derivation, closely packed terminally attached chains are expected to form a layer of thickness  $L$  that scales linearly with molecular weight and within which the segment density is nearly constant over most of the span of  $L$ . (It drops off in a power law fashion over a length scale  $\delta$  to about  $\sigma a^{-3}$  at the wall and exponentially to zero with decay length  $\delta$  at the solvent periphery of the layer.)

This line of reasoning could explain the extended range of forces we report here, if our adsorbed block copolymer layers resemble sufficiently terminally grafted chains at high surface density.<sup>28</sup> We can make a plausible argument that they do by modifying the above discussion to account for some aspects of block copolymer adsorption. We begin by asserting that the surface density  $\sigma$  of adsorption in our case is controlled by the PV2P block. In particular, let us assume that the block copolymer adsorbs to saturation, a condition defined by the point at which the PV2P blocks cover the entire surface with nonoverlapping, osculating, flattened disks of characteristic radius equal to  $R_{g,PV2P}$ , the radius

(28) de Gennes, P.-G. *Macromolecules* **1980**, *13*, 1069.

(29) Alexander, S. *J. Phys. (Paris)* **1977**, *38*, 983.

(30) Gast, A. P.; Leibler, L. *J. Phys. Chem.* **1986**, *89*, 3947.

(31) Flory, P. J. "Principles of Polymer Chemistry"; Cornell University Press: Ithaca, 1953.

(32) de Gennes, P.-G. *Scaling Concepts in Polymer Physics*; Cornell University Press: Ithaca, 1979.

(33) The term blob has become the standard terminology<sup>32</sup> for swollen portions of a polymer chain of some characteristic length scale in a polymer fluid.

of gyration of the PV2P block in toluene. At that point

$$\sigma = a^2/R_{g,PV2P}^2 \quad (12)$$

The condition for stretching of the PS block is given by (see eq 2)

$$\sigma a^2 R_{g,PS}^2 > 1 \quad (13)$$

or, substituting the result of eq 12

$$R_{g,PS}^2/R_{g,PV2P}^2 > 1 \quad (14)$$

This condition is clearly met in toluene which is a very good solvent for PS and a nonsolvent for PV2P. For example, we expect under good solvent conditions  $R_{g,PS} = a_{PS}N_{PS}^{3/5}$  and under nonsolvent conditions  $R_{g,PV2P} = a_{PV2P}N_{PV2P}^{1/3}$ . For the sake of a rough estimate, we can take the monomer sizes equal  $a_{PS} = a_{PV2P}$  and the monomer molecular weights equal so that for the 60/60 block copolymer, where  $N_{PS} \approx N_{PV2P} = N \approx 600$

$$R_{g,PS}^2/R_{g,PV2P}^2 \approx N^{8/15} \approx 30 \quad (15)$$

To put this argument most simply, we are saying that PV2P adsorbs tightly to saturation in a compressed configuration and, in so doing, squeezes the effectively terminally attached, nonadsorbing PS chains into stretched configurations. Equations 14 and 15 suggest that this will be the normal mode of block copolymer adsorption, for a pair with relative solvent and surface affinities like PS and PV2P in toluene on mica, as long as the surface-bound block is not significantly longer than the dangling block.

Detailed scrutiny of this argument, and its application to our experiments, requires, at a minimum, further data on the dependence of the  $F(D)$  curves on both PS and PV2P block molecular weights, as well as spectroscopic examination of the adsorbed PV2P block for more information on adsorbed amount and the configuration of the adsorbed PV2P. Work on both of these aspects is in progress. It is, however, possible to use this argument to examine our data quantitatively regarding the thickness of the dangling layer, or more specifically in our data, the range of the force vs. distance curves.

From eq 8 and 9, we see that

$$L = (N_{PS}/g)\delta \quad (16)$$

From eq 7, we have  $g = (\delta/a_{PS})^{5/3}$ . The essence of our argument leading up to eq 12 is that  $\delta \approx R_{g,PV2P}$ , so that making these two successive substitutions for  $g$  and  $\delta$  in eq 16 gives

$$L = N_{PS}a_{PS}^{5/3}R_{g,PV2P}^{-2/3} \quad (17)$$

Assuming again that  $a_{PS} = a_{PV2P} = a$ , and remembering that  $R_{g,PV2P} = aN_{PV2P}^{1/3}$ , our prediction for these layers is

$$L = aN_{PS}N_{PV2P}^{-2/9} \quad (18)$$

This can be compared with the contour length of the PS chain,  $L_c = aN_{PS}$ :

$$L/L_c = N_{PV2P}^{-2/9} \quad (19)$$

For  $N_{PV2P} = 600$ , as we have in the present experiments, we predict  $L/L_c = 0.24$ , in reasonably good agreement with our observation in the Results section that these PS chains are stretched to about 20% of their contour length.

The theoretical arguments do seem to be useful in interpreting these results and in planning new experiments. For example, eq 19 suggests that if we try to vary the surface density by varying the PV2P block molecular weight, we expect to see a rather weak dependence of  $L$  upon  $N_{PV2P}$ . For example, a 10-fold reduction of the PV2P molecular weight is expected to produce a 67% expansion in  $L$ . The scaling arguments, however, in no way obviate the need for a more detailed calculation of  $F(D)$  profile between adsorbed copolymer layers. This will be necessary in order to interpret the detailed forms of the curves, for example, possible power law behavior presented in Figures 6.

Figure 5 shows that just above  $T_\theta$  in these block copolymer layers, where bridging has been blocked by the PV2P layer, the

forces are purely repulsive. Homopolystyrene exhibits strong attractions under these same conditions.<sup>10</sup> This is decisive evidence of the role of bridging in homopolymer layers near  $T_\theta$ . The appearance of attraction on dropping the temperature below  $T_\theta$ , shown in Figure 6, enables us to estimate the portion of the attraction that comes from segmental mixing alone, by comparing the magnitude of the attraction here with that seen previously in homopolymers. The magnitude of the attractive force ten degrees below  $T_\theta$  with homopolystyrene in cyclohexane is about  $-500 \mu\text{N/m}$ .<sup>10</sup> Here we determine an attractive minimum about  $-100 \mu\text{N/m}$ , leading to the conclusion that bridging is the dominant source of attraction in the former case.<sup>10</sup> This is further supported by other measurements we have made of the adhesion between a simple PS adsorbed layer and bare mica gain in CH below  $T_\theta$ .<sup>34</sup> There, all adhesive attraction is due to bridging and the magnitude of the adhesion is more than ten times that between two PS surfaces under the same conditions.

Quantitative comparisons between these data and those of our previous work<sup>10</sup> must comprehend the fact that even under identical conditions of solvent and temperature there is considerably *more*-PS attached to the surface in the block copolymer experiments than in the homopolymer experiments. An estimate based on eq 12 gives the surface density,  $\sigma a^2$ , as about  $10^{17}$  chains/m<sup>2</sup> for 60K PV2P (assuming  $R_{g,PV2P} \approx 3.0 \text{ nm}$ ). This corresponds to a weight density on the surface of about  $10 \text{ mg/m}^2$ , approximately three times higher than the homo-PS adsorbances in ref 10.

The range of the steep repulsion near  $T_\theta$  in Figures 5 and 6 is about  $3R_g$  to  $4R_g$  of the PS, which is extended significantly from the value of  $1R_g$  typically found for the onset of repulsion in PS near  $T_\theta$ .<sup>10</sup> This range, considerably reduced from about  $10R_g$  to about  $4R_g$  in going from toluene to cyclohexane, is due, we believe, to the near- $T_\theta$  condition of the latter case. Near  $T_\theta$ , binary segmental interactions have small effect,<sup>31,32</sup> so that the first partial overlap of the PS layers may produce negligible observable interaction. The swelling of the surface-constrained layers is weaker near  $T_\theta$ , as well.

Modification of eq 19 to the case of the eq 19 to the case of the near- $T_\theta$  condition (where  $g = \delta/a_{PS}$ )<sup>31,32</sup> leads to

$$L/L_c = N_{PV2P}^{-1/3} \quad (20)$$

For our case of  $N_{PV2P} = 600$  this gives  $L/L_c = 0.12$ , compared with 0.24 in toluene, in reasonable concert with our observation of the range reduction of the forces from  $10R_g$  to  $4R_g$  an exchange of a good PS solvent for a  $\theta$  solvent.

Our conclusion from the examination of the data based on these simple quantitative arguments is that they do indeed provide a reasonable, unified explanation of the data. The weak points in the case as it stands right now are the lack of sufficient data to examine adequately the molecular weight scaling laws we have suggested and the lack of a more detailed theory of the force profiles between the plates. The ratio of ranges of forces for the two copolymers is slightly greater than linear in PS block molecular weight. The  $F(D)$  curves are not clean power laws.<sup>8</sup> Whether these observations arise from some experimental imperfection, such as the slight, but nonnegligible, polydispersity of our 60/150 sample, or whether they represent some physical chemistry of the layers yet to be understood awaits our further experimentation and theoretical analysis.

### Concluding Remarks

This work has shown that the forces between two bound layers of polymer immersed in a good solvent for the polymer are repulsive. Block copolymer layers such as we have studied, with one compact, tightly bound block and one solvent-swollen, unbound block, are demonstrated by our work to adopt adsorbed configurations where the unbound block is stretched away from the

(34) Granick, S.; Patel, S.; Tirrell, M. *Nature (London)*, submitted.

(35) Leibler, L.; Orland, H.; Wheeler, J. C. *J. Chem. Phys.* **1983**, *79*, 3550.

(36) Selb, J.; Marie, P.; Rameau, A.; Duplessix, R.; Gallot, Y. *Polym. Bull.* **1983**, *10*, 444.

(37) Whitmore, M. D.; Noolandi, J. *Macromolecules* **1985**, *18*, 657.



surface. The forces measured between these layers do not conform obviously or closely to predictions made for irreversibly adsorbed homopolymer layers immersed in good solvents. On the other hand, a rather simple adaptation of the Alexander–de Gennes theory<sup>28,29</sup> of terminally attached chains to the case of block copolymers provides a coherent interpretation of our force measurements.

A more complete theory of the  $F(D)$  curves, enabling prediction of the magnitude of  $F$  at a certain  $D$ , will be difficult to accomplish without more detailed knowledge of the configuration of the molecules in the adsorbed layer, via means independent from the inferences we have made here from the surface forces measurement. For example, it is not known from any direct measurement whether, when these two copolymer layers are brought together, the PS chains initially compress or interpenetrate. The very limited lateral mobility of these chains and the step-function-like shape<sup>28–30</sup> of the segment density profile in these swollen layers of high surface density argue against interpenetration. Direct spectroscopic investigation of the molecular configuration and degree of segmental mixing between the layers when they are brought together would be very valuable to the interpenetration. A photophysical technique such as fluorescence quenching or energy transfer may be useful.

In a more general vein, the application of surface forces measurement between polymer layers has, we believe, great potential to resolve some fundamental problems in adhesion, surface

chemistry, and structured fluids, such as block copolymer–homopolymer blends,<sup>30,35–37</sup> that exhibit a rich variety of phase behavior.

**Acknowledgment.** We gratefully acknowledge the contributions of Patricia M. Cotts of IBM to the work of characterizing these copolymers. Financial support of this work at the University of Minnesota was provided by the National Science Foundation, Polymers Program (NSF-DMR 81-15733 and 85-01018), and by an IBM Polymer Fellowship to Sanjay Patel. The work on surface forces at Minnesota owes much to Jacob Israelachvili of the Australian National University, who supervised the construction of our apparatus at ANU and generously assisted us at an early stage in establishing our own measurement capability. In this connection we acknowledge, too, important assistance from Roger Horn and Richard Pashley (ANU). We are grateful to Phil Pincus (UCSB), Jacob Klein (Weizmann Institute), Bill Russel (Princeton), and Pierre-Gilles de Gennes (Collège de France) for critical discussion concerning this work.

**Registry No.** (PV2P)(PS) (copolymer), 24980-54-9.

**Supplementary Material Available:** A 3-page description of the experimental technique, including a diagram of the apparatus (Figure A), and three tables including the data of Figures 2–6 (7 pages). Ordering information is given on any current masthead page.

## Test of Variational Transition State Theory and Multidimensional Semiclassical Transmission Coefficient Methods against Accurate Quantal Rate Constants for $H + H_2/HD$ , $D + H_2$ , and $O + H_2/D_2/HD$ , Including Intra- and Intermolecular Kinetic Isotope Effects

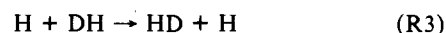
Bruce C. Garrett,<sup>†</sup> Donald G. Truhlar,<sup>\*‡</sup> and George C. Schatz<sup>\*±</sup>

*Contribution from the Chemical Dynamics Corporation, Columbus, Ohio 43220, the Department of Chemistry, University of Minnesota, Minneapolis, Minnesota 55455, and the Department of Chemistry, Northwestern University, Evanston, Illinois 60201. Received September 27, 1985*

**Abstract:** Rate constants and kinetic isotope effects for the title reactions have been calculated by using accurate quantum dynamical methods and used to test the accuracy of corresponding rate constants from conventional and variational transition state theory. The quantum dynamical rate constants are estimated to be within 35% of the exact rate constants for the potential surfaces chosen for this comparison. For all the reactions considered, the conventional and variational transition state theory rate constants with unit transmission coefficient are found to be very close to each other (better than 7%) but in poor agreement with the accurate quantum results (off by factors of 6–22 at 300 K). This indicates that although variational effects are small, tunnelling makes a very important contribution to the rate constants, and it is found that this tunnelling contribution is described quantitatively for all the reactions considered with use of the least action ground state (LAG) transmission coefficient. The combination of improved canonical variational theory (ICVT) and LAG yields rate constants which have an average error (considering all the reactions and temperatures studied) of 15% compared to the accurate quantum rate constants, and in only one case ( $D + H_2$  at 200 K) does the ICVT/LAG rate constant differ by more than 35% from the accurate value. The comparison of ICVT/LAG kinetic isotope effects is found to be similarly good, with the worst comparisons occurring for intramolecular ( $X + HD$ ) isotope ratios.

### I. Introduction

Recent advances in quantal reactive scattering methods have made it possible to calculate rate constants without dynamical approximations for two series of isotopically related reactions:<sup>1,2</sup>



and

<sup>†</sup>Chemical Dynamics Corp.

<sup>‡</sup>University of Minnesota.

<sup>±</sup>Northwestern University.